

MIMO WIRELESS MULTIPATH RAY PARAMETER ESTIMATION FROM CHANNEL TRANSFER MATRIX MEASUREMENTS

Brian D. Jeffs and Jon Wallace

Brigham Young University, Department of Electrical and Computer Engineering
459 CB, Provo, UT 84602, email: bjeffs@ee.byu.edu

ABSTRACT

In MIMO wireless communication using space-time coding techniques, it is important to understand channel characteristics so that optimum coding schemes, array configurations, and performance analysis can be developed. Increasingly, understanding of MIMO channels is being aided by direct channel probing experiments to measure transfer matrix, \mathbf{H} . An alternate channel representation based on propagating ray parameters has many advantages. We propose an algorithm to compute high precision estimates of channel ray parameters directly from \mathbf{H} measurements. Examples are presented where rays are identified, and departure angles, arrival angles, and complex path gains are estimated.

1. INTRODUCTION

As the field of Multiple Input, Multiple output (MIMO) wireless communications develops, with its promise of dramatic capacity improvements, it becomes important to understand the characteristics of the real-world MIMO channel. Accurate channel models based on channel probing measurements are crucial in developing new space-time coding schemes and analyzing their performance. A number of researchers are reporting experiments where the MIMO channel transfer matrix, \mathbf{H} , is being measured for specific antenna arrays [1, 2]. In other work, a specular scattering parametric ray model is adopted and probing systems have been used to estimate individual ray parameters [3, 4, 5, 6].

These two representations are both useful for channel probing, and each has advantages. \mathbf{H} is eminently usable in designing space-time coding schemes and channel capacity calculations. From an experimental channel probing perspective, \mathbf{H} is easier to measure directly (and in less time) than are the ray parameters [1, 2, 7, 3]. However, the parametric ray model, which we designate $C(\phi, \theta)$, is more closely tied to the physical channel properties. It is a lower dimensional representation, and is therefore better suited for parametric, or statistical channel modeling efforts. The ray model is easily interpreted in terms of the physical scattering objects present in a channel. Perhaps more importantly, given $C(\phi, \theta)$, it is possible to compute \mathbf{H} for any array configuration, not just the one used in probing measurements [3].

This paper presents an algorithm which can compute, from an observed \mathbf{H} matrix, precision estimates of the underlying ray departure and arrival angles and path gains. Some researchers have reported excellent work in estimating ray parameters using antenna array probing systems [4, 5, 6]. As compared with these methods, the proposed algorithm has the following advantages: 1) Estimates

This project was supported by National Science Foundation grant number CCR-9979452.

are formed directly from \mathbf{H} measured with *arbitrary* arrays; special array configurations for channel sounding are not required. An \mathbf{H} matrix estimated as part of a space-time coding channel estimation process can be used directly to obtain ray parameters. 2) No spatial smoothing is required for rank enhancement, so more rays can be identified for a given array size. 3) No beamforming, with its inherent resolution limitations, is required.

1.1. Channel Ray Model

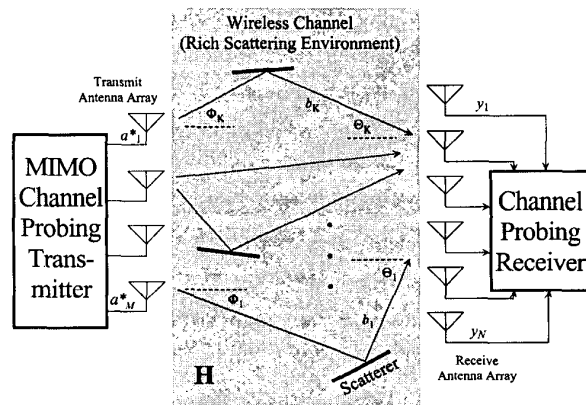


Fig. 1. Illustration of MIMO wireless propagation in a multipath environment. Individual ray paths in channel model $C(\phi, \theta)$ are shown with departure and arrival angles (Φ_k and Θ_k) and complex path gains, (b_k). The corresponding channel transfer matrix, \mathbf{H} , is an alternate model formed as a superposition of array responses induced by the multipath rays.

Figure 1 illustrates the MIMO propagation channel. We assume propagation in the horizontal plane only, flat fading, and specular scattering. The method described below however can be extended in the obvious way to 3-D propagation with scattered rays in a volume rather than a plane.

The channel ray statistical model is based on Spencer's [7], which is an extension of [8]. To the Spencer model we add a ray departure angle, θ , and drop the time of arrival terms since we are dealing with narrowband flat fading communications. The channel

is represented as a sum of discrete ray paths:

$$C(\phi, \theta) = \sum_{k=1}^K b_k \delta(\phi - \Phi_k, \theta - \Theta_k), \quad (1)$$

where Φ_k and Θ_k are the departure and arrival angles respectively for the k^{th} ray in the channel from transmit to receive array. As in [7], Φ_k and Θ_k are realized as random variables with a mixture of uniform and Laplacian distributions based on a cluster model. Complex ray path gain, $b_k = \beta_k e^{j\psi_k}$. β_k is Rayleigh distributed with a random mean drawn from a double exponential distribution, and ψ_k is uniform $(0, 2\pi)$.

The MIMO narrowband transfer matrix, \mathbf{H} , relates the complex transmit array excitation vector, \mathbf{a} , to the observed receiver array element response vector, \mathbf{y} , as $\mathbf{y} = \mathbf{H}\mathbf{a}^*$, where $*$ indicates complex conjugate. One can compute \mathbf{H} in a straightforward manner from $C(\phi, \theta)$ for any given transmit and receive array configuration.

$$\begin{aligned} \mathbf{H} &= \sum_{k=1}^K b_k \mathbf{q}(\Theta_k) \mathbf{w}(\Phi_k)^H, \text{ where} \quad (2) \\ \mathbf{q}(\theta) &= [\mathbf{d}_r(\theta) \odot \mathbf{v}_r(\theta)]^T, \\ \mathbf{w}(\phi) &= [\mathbf{d}_t(\phi) \odot \mathbf{v}_t(\phi)]^T, \\ \mathbf{v}_r(\theta) &= [e^{j\frac{\omega}{c}\tilde{r}_1 \cdot \tilde{s}_\theta}, \dots, e^{j\frac{\omega}{c}\tilde{r}_L \cdot \tilde{s}_\theta}]^T, \\ \tilde{s}_\theta &= \hat{i} \cos \theta + \hat{j} \sin \theta. \end{aligned}$$

where \odot indicates the element-wise Schur matrix product, H is complex conjugate transpose, and \cdot is the inner product of 3-D vectors. \tilde{r}_l and \tilde{r}_l are the 3-D position vectors for the l^{th} elements of the transmit and receive arrays respectively. $\mathbf{v}_r(\phi)$ is the receive array steering vector for direction θ (i.e. array response to a unit plane wave from direction θ), $\mathbf{d}_r(\theta)$ is the vector of individual antenna element directional responses, and \hat{i} and \hat{j} are unit vectors along x and y axes respectively. $\mathbf{v}_t(\phi)$, \tilde{s}_ϕ , and $\mathbf{d}_t(\phi)$ are defined similarly.

Though the forward relationship of equation (2) is readily computed, it is the inverse relationship of finding $C(\phi, \theta)$ from \mathbf{H} which is of interest here. The following section presents an approach to solve this ill-posed inverse problem.

2. AN ALGORITHM FOR RAY PARAMETER ESTIMATION

The problem addressed in this section is as follows: given an observed \mathbf{H} obtained from a channel probing experiment, estimate the number of multipath rays, K , and ray parameters Φ_k , Θ_k , β_k and ψ_k for each ray. If excitation vector, \mathbf{a} is length N (i.e. N elements in the transmit array), and receive vector \mathbf{y} is length M , then $\text{rank}\{\mathbf{H}\} \leq \min(M, N)$ serves as an upper bound on the number of individual rays that can be identified. The algorithm presented here uses a MUSIC-like subspace decomposition approach and can identify up to $\min(M, N) - 1$ rays. This requires that the probing arrays have more antenna elements than the expected number of multipaths, which for rich scattering environments implies that the arrays must be of significant size. We have developed a direct \mathbf{H} indoor channel probing system that supports up to 16 element arrays at each end. This is described in a following section.

A high resolution angle of arrival estimation algorithm is required. Not only do we anticipate channel rays to be in tightly

spaced clusters [7], but experiments have shown that even for a simple case of three widely spaced rays, the obvious ‘‘matched filter’’ 2-D beamformer peak picking approach,

$$[\hat{\Phi}_k, \hat{\Theta}_k] = \arg k^{\text{th}} \text{ local } \max_{\phi, \theta} \mathbf{q}(\theta)^H \mathbf{H} \mathbf{w}(\phi), \quad (3)$$

is unreliable, and often resolves only the strongest ray.

The proposed algorithm consists of two phases. In phase one, high resolution estimates are made separately for the ray angles of departure from the transmit array, and angles of arrival at the receive array. In phase two, corresponding departure and arrival angle pairs are matched for each multipath ray, and complex ray path gain is computed. For phase one, we express equation (2) in matrix form and explicitly include the observation noise term, \mathbf{N} ,

$$\begin{aligned} \mathbf{H} &= \mathbf{Q} \mathbf{B} \mathbf{W}^H + \mathbf{N}, \text{ where} \quad (4) \\ \mathbf{Q} &= [\mathbf{q}(\Theta_1), \dots, \mathbf{q}(\Theta_K)], \\ \mathbf{W} &= [\mathbf{w}(\Phi_1), \dots, \mathbf{w}(\Phi_K)], \\ \mathbf{B} &= \text{diag}\{\mathbf{b}\}, \mathbf{b} = [b_1, \dots, b_K]^T. \end{aligned}$$

\mathbf{H} can also be represented by its singular value decomposition,

$$\mathbf{H} = [\mathbf{U}_s | \mathbf{U}_n] \Lambda [\mathbf{V}_s | \mathbf{V}_n]^H, \quad (5)$$

where subscript ‘ s ’ indicates the partition of singular vectors corresponding to the signal subspace, i.e. those with significant eigenvalues in diagonal Λ . Subscript ‘ n ’ indicates the noise subspace, and noise dominant singular values.

\mathbf{U}_s spans the same space as \mathbf{Q} , and is orthogonal to \mathbf{U}_n . Likewise, \mathbf{V}_s has the same span as \mathbf{W} . Thus MUSIC scans for both ray departure and arrival angles can be formed, and ray angles estimated as shown in the Phase I algorithm description below. False (extra) peaks can occur with a MUSIC scan, but are resolved in phase II.

We note that for certain probing array geometries where antennas can be grouped into two identical sub arrays, an ESPRIT [4, 5] approach could be used for phase one. ESPRIT may be preferred, if array geometry restrictions are tolerable, because of its more desirable angle estimation properties. The method presented here is more general.

In phase II the correspondence between $\hat{\Phi}_k$ and $\hat{\Theta}_l$ estimates must be established, and complex ray gains, b_k estimated. The correspondence problem is non-trivial because a channel with K rays has $K!$ distinct possible pairings of indices k and l . Given $\hat{\Phi}_k$ and $\hat{\Theta}_l$ and assuming i.i.d. Gaussian measurement noise, the maximum likelihood estimate for pairings and ray gains is,

$$\begin{aligned} [\hat{\mathbf{B}}, \hat{\mathbf{P}}] &= \arg \min_{\mathbf{B}, \mathbf{P}} \|\mathbf{H} - \hat{\mathbf{Q}} \mathbf{P} \mathbf{B} \hat{\mathbf{W}}^H\|_F^2, \text{ such that,} \\ \mathbf{P} &= \begin{bmatrix} 0 & \dots & 0 & 1 & 0 & \dots & 0 \\ \vdots & & & \ddots & & & \end{bmatrix}, \quad (6) \end{aligned}$$

where \mathbf{B} is constrained to be diagonal and \mathbf{P} is a permutation matrix with each row and column containing at most one ‘1’. Placement of these ‘1’s associates columns of $\hat{\mathbf{Q}}$ (and thus arrival angles, $\hat{\Theta}_k$) with columns of $\hat{\mathbf{W}}$ (i.e. $\hat{\Phi}_k$). $\hat{\mathbf{Q}}$ and $\hat{\mathbf{W}}$ are formed as in equation (5) but using phase I angle estimates, and without knowledge of correct column ordering. The difficulty with equation (6) is that the optimization criterion is not convex in \mathbf{P} , and therefore solution requires an exhaustive search over all $K!$ possible configurations for \mathbf{P} . The proposed algorithm dramatically

reduces the search space by limiting the number of candidate departure - arrival angle pairings.

Consider the least squares solution of equation (5) for unstructured \mathbf{B} (not forcing diagonality),

$$\hat{\mathbf{B}} = \hat{\mathbf{Q}}^\dagger \mathbf{H} (\hat{\mathbf{W}}^H)^\dagger, \quad (7)$$

where \dagger denotes matrix pseudo inverse. Observe that $\hat{\mathbf{B}} \approx \mathbf{P} \mathbf{B}$, where the approximation is due only to estimation errors in $\hat{\Phi}_k$ and $\hat{\Theta}_k$, and array calibration errors. Neglecting these errors, $\hat{\mathbf{B}}$ would have non-zero elements only at locations corresponding the '1's in matrix \mathbf{P} , and can thus serve to identify \mathbf{P} and match departure and arrival angle pairs. If \mathbf{P} is known and \mathbf{B} is constrained to be diagonal, then the solution to equation (6) reduces to the closed form

$$\begin{aligned} \mathbf{b} &= \mathcal{A}^\dagger \mathbf{h}, \\ \mathbf{h} &= \text{vec}\{\mathbf{H}\} \\ \mathcal{A} &= [\mathbf{w}_1^* \otimes \mathbf{Q} \mathbf{p}_1 | \cdots | \mathbf{w}_K^* \otimes \mathbf{Q} \mathbf{p}_K], \end{aligned} \quad (8)$$

where \otimes is the Kronecker matrix product, and \mathbf{w}_k and \mathbf{p}_k indicate the k^{th} columns of \mathbf{W} and \mathbf{P} respectively. The phase II algorithm described below exploits these relationships and uses a short interaction to solve equation (6) in the presence of error in $\hat{\mathbf{B}}$.

ALGORITHM STEPS, Phase I

1. Compute partitioned SVD matrices of \mathbf{H} , \mathbf{U}_n and \mathbf{V}_n , as in equation (5).
2. Compute MUSIC spectra for departure and arrival angles as

$$\begin{aligned} S_t(\phi) &= \frac{1}{\|\mathbf{w}(\phi)^H \mathbf{V}_n\|_2^2}, \\ S_r(\theta) &= \frac{1}{\|\mathbf{q}(\theta)^H \mathbf{U}_n\|_2^2}, \end{aligned} \quad (9)$$

using a dense sampling in ϕ and θ (e.g. 0.1 degree sample increments).

3. Form uncoupled estimates separately for ray departure and arrival angles corresponding to local MUSIC spectrum peaks.

$$\begin{aligned} \hat{\Phi}_k &= \arg k^{\text{th}} \text{ local } \max_{\phi} S_t(\phi), \\ \hat{\Theta}_l &= \arg l^{\text{th}} \text{ local } \max_{\theta} S_r(\theta). \end{aligned} \quad (10)$$

Phase II

1. Compute unstructured $\hat{\mathbf{B}}$ as in equation (7).
2. Define T as a threshold value such that $2K$ elements, $\hat{b}_{k,l}$, of $\hat{\mathbf{B}}$ have magnitudes greater than T . Let

$$\hat{\mathbf{P}} = \{\hat{p}_{k,l}\}, \text{ where } \hat{p}_{k,l} = \begin{cases} 1 & |\hat{b}_{k,l}| \geq T \\ 0 & \text{Otherwise} \end{cases}. \quad (11)$$

In other words, non zero entries in $\hat{\mathbf{P}}$ correspond to the $2K$ largest elements of $\hat{\mathbf{B}}$. These are candidate ray angle pairs.

3. Repeat the following steps K times.

- (a) Find the ray departure arrival angle pair that contributes least to reducing error in the forward modeled \mathbf{H} . Using equation (8) to solve for \mathbf{B} for each (k, l) pair in the minimization, find

$$(k', l') = \arg \min_{(k,l) \in S, B} \|\mathbf{H} - \hat{\mathbf{Q}} \mathbf{P} \mathbf{B} \hat{\mathbf{W}}^H\|_F^2,$$

where $S = \{\forall (k, l) | p_{k,l} = 1\}$.

- (b) Remove this pair from $\hat{\mathbf{P}}$, i.e. $p_{k',l'} = 0$.

4. The final \mathbf{P} contains the K correct ray angle pairings, and is used in equation (8) for the final estimate of \mathbf{b} .

In the preceding discussion, it was assumed that the number of rays, K , was known. Of course, K must be estimated. This could be done using standard model order estimation techniques, such as the Minimum Description Length, or the Akaike Information Criterion. However, excellent results were obtained by simply repeating the algorithm above with increasing values of K . Incrementing K is stopped when the error norm computed in Phase II step 3 a) fails to decrease with increasing K .

3. SIMULATED RESULTS

Figures 2 and 3 present test results for two cases of simulated \mathbf{H} probing measurements. The channels were synthesized as random samples of the statistical ray model in [7]. From the channel description, $C(\phi, \theta)$, equation (2) was used, with added noise, to form \mathbf{H} . A carrier frequency of 6.0 GHz was used (to permit comparisons with previous direct ray probing measurements using narrow beam dish antennas [3]). Both transmit and receive arrays consisted of 13 vertical monopoles arranged in a symmetric cross configuration in the horizontal plane. Uniform inter-element spacing between neighboring elements was 0.05m (1.0 λ). This array design permits resolving up to 12 rays, and eliminates the front-back ambiguity encountered with a uniform line array. As seen in the figures, excellent ray parameter estimates were obtained.

Figure 4 shows the transmitter half of a probing system we have developed for directly measuring \mathbf{H} for antenna arrays of up to 16 elements each. We have collected an number of data sets in the 2.4 GHz band using patch antenna and $\frac{1}{4}\lambda$ spaced vertical monopole arrays. We are in the process of developing precision array response calibration techniques so that these \mathbf{H} measurements can be used in the high resolution ray parameter estimation algorithm presented here.

The proposed algorithm has proved to be very reliable in a wide range of trials with synthesized \mathbf{H} . It degrades gracefully with increasing noise level, which is sometimes not the case for high resolution DOA estimation methods. The next step in our studies is to process real-world probe data from our test platform. This will require better array phase and gain calibration than currently available. We are developing an in situ self calibration method based on Bayesian optimization assuming a sparse point-like distribution for ray angles.

4. REFERENCES

- [1] J.W. Wallace and Michael A. Jensen, "Spatial characteristics of the mimo wireless channel: Experimental data acquisition and analysis," in *IEEE International Conference on Acoustics, Speech, and Signal Processing*, Salt Lake City, May 2001, vol. IV, pp. 2497-2500.

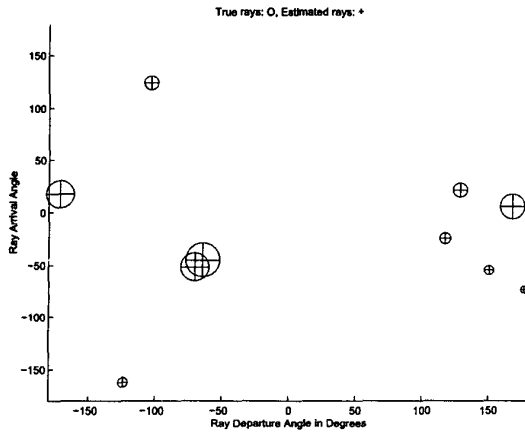


Fig. 2. Demonstration of ray parameter estimation algorithm performance. A synthetic noiseless \mathbf{H} probing matrix was generated from the rays shown by the circles. Each circle is centered on the grid point corresponding to its departure and arrival angle pair. Circle diameter is proportional to path gain magnitude, β_k . Crosses indicate estimated ray angles, and amplitudes computed from \mathbf{H} . The number of rays was correctly estimated at 10, and very good angle and gain matches were achieved.

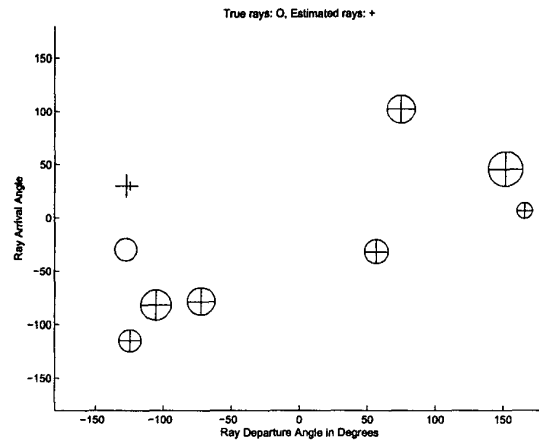


Fig. 3. Ray parameter estimation with 45 dB SNR in the synthetic \mathbf{H} probing matrix. This SNR level is commonly achieved with the probing test platform described in Figure 4. Nine rays were found; the actual channel had eight. One arrival angle was mis-estimated but the others show good correspondence.

- [2] M. Nilsson, B. Völcker, and B. Ottersten, "A cluster approach to spatio-temporal channel estimation," in *IEEE International Conference on Acoustics, Speech, and Signal Processing*, Istanbul, Turkey, Apr. 2000, vol. V, pp. 2757–2760.
- [3] B.D. Jeffs, E. Pyper, and B. Hunter, "A wireless mimo channel probing approach for arbitrary antenna arrays," in *IEEE International Conference on Acoustics, Speech, and Signal Processing*, Salt Lake City, May 2001, vol. IV, pp. 2493–2496.
- [4] M. Steinbauer, A.F. Molisch, and E. Bonek, "The double-directional radio channel," *IEEE Antennas and Propagation Magazine*, vol. 43, no. 4, pp. 51–63, Aug. 2001.
- [5] A. Richter, D. Hampicke, G. Sommerkorn, and R.S. Thomä, "Joint estimation of dop, time-delay, and doa for high-resolution channel sounding," in *IEEE Vehicular Technology Conference, VTC2000*, Boston, Sept. 2000, pp. 1045–1049.
- [6] D. Hampicke, Ch. Schneider, M. Landmann, A. Richter, G. Sommerkorn, and R.S. Thomä, "Measurement-based simulation of mobile radio channels with multiple antennas using a directional parametric data model," in *IEEE Vehicular Technology Conference, VTC2001*, Atlantic City, Oct. 2001, pp. 1045–1049.
- [7] Q.H. Spencer, B.D. Jeffs, M.A. Jensen, and A.L. Swindlehurst, "Modeling the statistical time and angle of arrival characteristics of an indoor multipath channel," *IEEE Journal on Selected Areas in Communications*, vol. 18, no. 3, pp. 347–360, Mar. 2000.
- [8] A.A.M. Saleh and R.A. Valenzuela, "A statistical model for indoor multipath propagation," *IEEE Journal on Selected Areas in Communications*, vol. SAC-5, pp. 128–135, Feb. 1987.

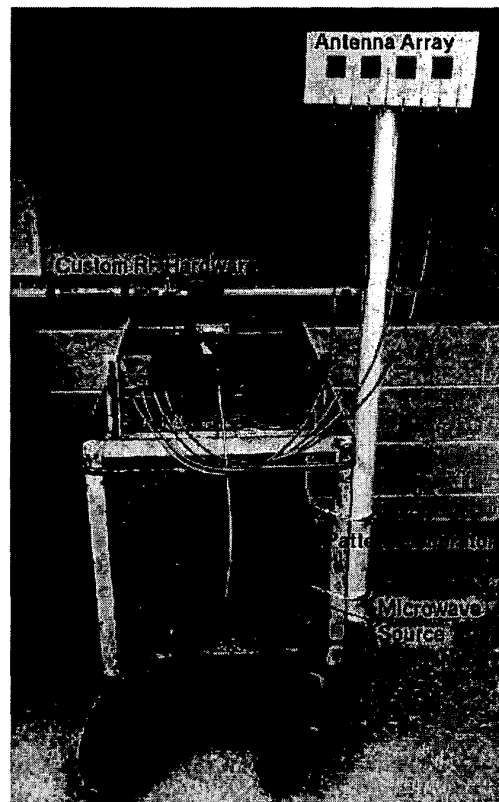


Fig. 4. Transmitter section of the MIMO channel probe system. This system can directly measure \mathbf{H} between two indoor sites for arrays as large as 16×16 elements.